PHYSICAL REVIEW E **95**, 060601(R) (2017)

Ultra-long-range dynamic correlations in a microscopic model for aging gels

Pinaki Chaudhuri[1] and Ludovic Berthier[2]
[1]*The Institute of Mathematical Sciences, C.I.T. Campus, Taramani, Chennai 600 113, India*
[2]*Laboratoire Charles Coulomb, UMR 5221, Université Montpellier and CNRS, 34095 Montpellier, France*
(Received 29 June 2016; revised manuscript received 10 February 2017; published 15 June 2017)

We use large-scale computer simulations to explore the nonequilibrium aging dynamics in a microscopic model for colloidal gels. We find that gelation resulting from a kinetically arrested phase separation is accompanied by "anomalous" particle dynamics revealed by superdiffusive particle motion and compressed exponential relaxation of time correlation functions. Spatiotemporal analysis of the dynamics reveals intermittent heterogeneities producing spatial correlations over extremely large length scales. Our study is a microscopically resolved model reproducing all features of the spontaneous aging dynamics observed experimentally in soft materials.

DOI: 10.1103/PhysRevE.95.060601

Understanding the complex mechanisms underlying the formation and stability of colloidal gels remains a challenge, despite the diversity of existing applications exploiting their mechanical properties. Gels are low-density structures forming percolating networks, with permanent or transient bonds [1–6]. A prevalent method to form physical gels follows a nonequilibrium route by quenching a homogeneous fluid into a phase coexistence region [1,7–12], which generates bicontinuous structures. When the dense phase forms an amorphous solid, the phase separation is kinetically hindered [13–16] and a gel forms. The dynamical and structural properties of these nonequilibrium gels slowly age with time.

This aging dynamics has been the subject of several experimental studies, which established that aging in colloidal gels is "anomalous" [17,18], since it differs qualitatively from the aging observed in conventional glassy materials [19,20]. Scattering experiments [21–25] report that time correlation functions are described by *compressed exponential* relaxations. This differs from the (exponential) diffusive dynamics in simple liquids or the (stretched exponential) decay observed in glassy fluids [26]. In addition, compressed exponentials emerge for *large enough displacements*, with the relaxation time scale $\tau(q)$ crossing over from $\tau \sim q^{-2}$, characteristics of a diffusive process, to $\tau \sim q^{-1}$, characteristic of ballistic dynamics, with decreasing the scattering wave vector q. Finally, spatially resolved dynamic measurements revealed the existence of *"ultra-long-ranged" correlations* extending up to the system size [27,28], again contrasting with the much smaller-ranged dynamic heterogeneity observed in glassy materials [29]. Such peculiar behavior is hypothesized to follow from the infrequent release of "internal stresses" that relax the gel network [18], but this is not supported by direct observation.

This overall phenomenology has been reported for a large class of soft materials [18], but it crucially lacks a fundamental understanding. To study this problem theoretically, one needs a model with a realistic gel structure, studied for large enough time scales to observe the slow dynamics, and over large enough length scales to detect long-ranged correlations. These three challenges have not been addressed before. There have been extensive studies of aging effects in particle-based computer simulations of dense glassy systems (e.g., [30,31]), but none of the above anomalous signatures are observed. For nonequilibrium gelation, the focus has been mainly on the formation of arrested structures via quenches into the phase-coexistence region, with little insight into the aging dynamics. On the other hand, in an equilibrium gel, compressed exponentials in the time correlations were reported, where they have a different nature [32,33]. Compressed relaxations were found in the case of mechanically induced coarsening, albeit at zero temperature [34]. More recent work [35] showed that local ruptures of a gel network at zero temperature can produce such compressed exponential relaxations, but they disappear at finite temperatures, similar to the results of Ref. [36]. Using a coarse-grained approach, it was suggested that localized bond-breaking events in gels may result in compressed exponentials [37], as recently observed in an elastoplastic model for glasses [38].

Using large-scale numerical simulations of a particle-based model for gel formation [13,14], we show that the spontaneous microscopic aging dynamics during gelation possesses all anomalous signatures reported experimentally. We find a subdiffusive aging dynamics at short length scales, corresponding to caged particle motion inside the gel strands, crossing over to superdiffusive relaxation at larger length scales triggered by intermittent snapping of the network. These relaxation events result in compressed exponential relaxations at small enough scattering vectors and correspond also to dynamic correlation length scales that are much larger than the typical pore size of the gel. These results thus provide a coherent microscopic picture of the anomalous aging dynamics observed experimentally.

Following [13,14], we study the properties of a binary Lennard-Jones mixture after it is suddenly quenched into its liquid-gas coexistence region. Although colloidal systems are often modeled using attractive forces that are shorter ranged, the main features of gelation are captured by this model [14]. To access large-enough system sizes, we work in two spatial dimensions. We consider a 65:35 A-B Lennard-Jones mixture with model parameters as in Ref. [39]. Because of its glass-forming ability, phase separation is kinetically hindered, which results in gelation. We perform molecular dynamics simulations using LAMMPS [40]. In our simulations, energies and lengths are expressed in Lennard-Jones units of interaction energy ϵ_{AA} and diameter σ_{AA} for the majority species. Particles have equal masses, m, and the time unit is $\sqrt{m\sigma_{AA}^2/\epsilon_{AA}}$.

In these reduced units, we observe incomplete phase separation of the binary mixture when temperature is lower

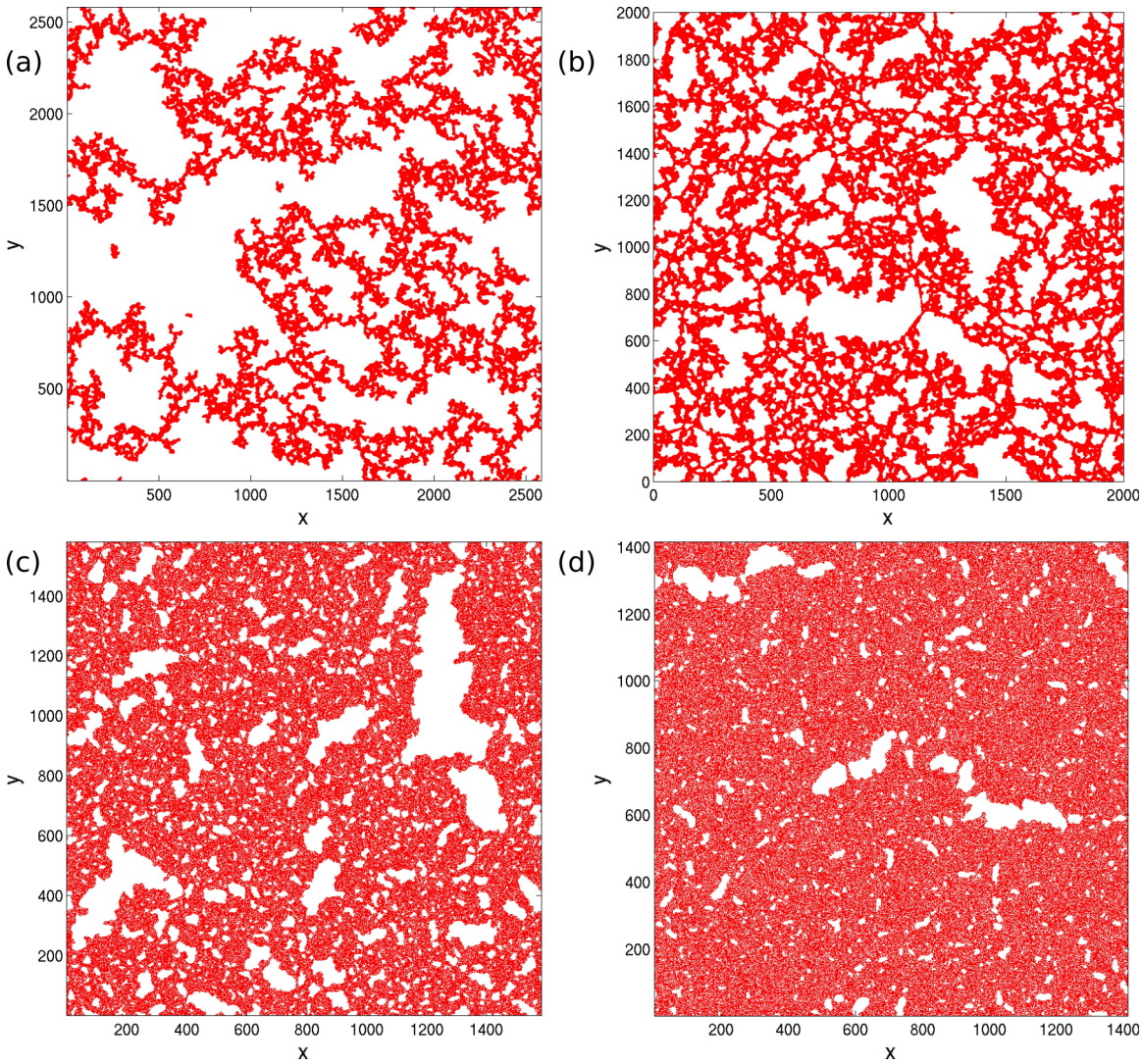

FIG. 1. Snapshots of the two-dimensional binary Lennard-Jones mixture at large time, $t = 2.7 \times 10^4$, following a quench from $T = 3.0$ to $T = 0.15$ at various densities (a) $\rho = 0.3$, (b) $\rho = 0.5$, (c) $\rho = 0.8$, and (d) $\rho = 1.0$.

than $T \approx 0.3$, and a bicontinuous structure is obtained for number densities in the range $0.25 < \rho < 1.1$. Our strategy is to first equilibrate the system at high temperature in the homogeneous region, $T = 3.0$, for different densities $\rho =$ 0.4, 0.5, 0.6, 0.7, 0.8, and 1.0. Then, at time $t = 0$, we instantaneously quench the system to low temperatures in the phase coexistence region, $T = 0.05$, 0.10, 0.15, 0.20, 0.30, 0.40, and 0.50. Thereafter, we follow the dynamical properties of the system at these different state points. In order to explore spatial correlations we study large systems ranging from $N = 10^4$ to 2×10^6 particles. A majority of the results shown below correspond to $N = 5 \times 10^5$. All data are averaged over at least four different initial conditions, which allows us to confirm that sample to sample fluctuations are small. During the dynamics, the temperature control is done via dissipative particle dynamics (DPD) thermostat [41], using a friction coefficient value of $\xi = 1$; tests performed with larger damping $\xi = 3, 10$ (but identical spatial range of dissipation) showed qualitatively similar results.

The nearly-arrested bicontinuous structures formed at large times for $T = 0.15$ and various densities are shown in Fig. 1, for a system with $N = 2 \times 10^6$. These images reveal the coexistence of a connected network of dense amorphous domains and empty pores. For $\rho = 0.3, 0.5$, the denser regions form a network with tenuous links, having a morphology reminiscent of those seen in experiments. At higher densities, $\rho = 0.8, 1.0$, the voids shrink and the dense domains become more compact. At higher temperatures, $T > 0.3$, these structures rapidly coarsen until complete phase separation. On the other hand, at very low temperatures, the gelation process is essentially arrested, because the particle bonds become nearly permanent. A detailed characterization of the gel structure can be found in [14]. Below, we explore the intermediate, experimentally relevant regime where the gel evolves very slowly with time, focusing on the temperature $T = 0.15$.

We study the microscopic dynamics as a function of the time t_w spent since gelation started. Such t_w dependence is demonstrated in Fig. 2(a) for the mean-squared displacements, $\Delta^2(t, t_w) = \frac{1}{N_A} \sum \langle |\mathbf{r}_i(t) - \mathbf{r}_i(t_w)|^2 \rangle$, for the majority species (type-A particles), where $\mathbf{r}_i(t)$ represents the position of particle i at time t, and the brackets represent an average over initial conditions. The data in Fig. 2(a) reveal that

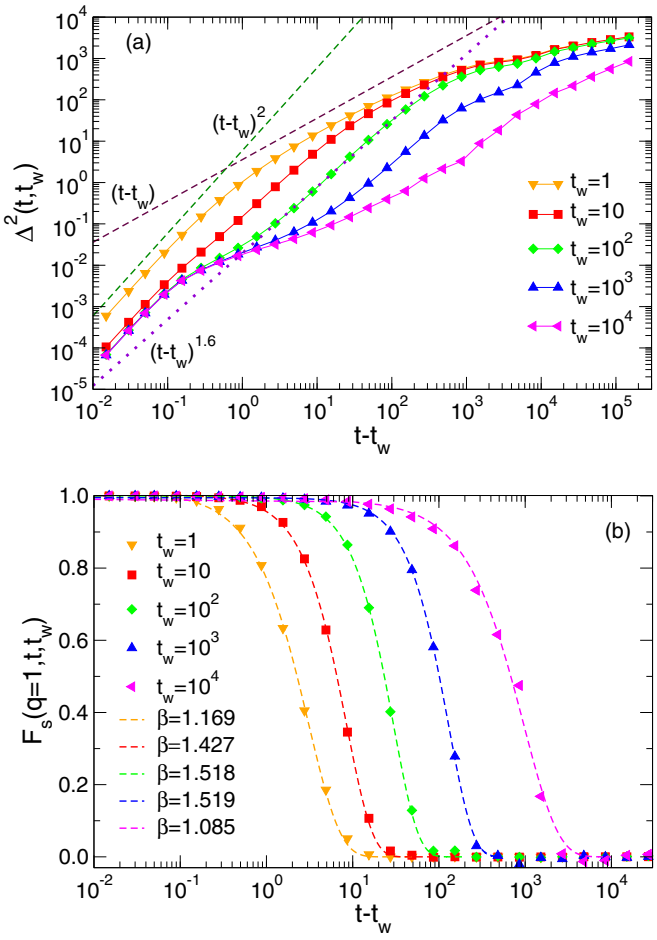

FIG. 2. $\rho = 0.5$, $T = 0.15$. (a) Mean-squared displacements, $\Delta^2(t,t_w)$, measured for different ages, t_w. A succession of ballistic, subdiffusive caging, superdiffusive cage escape, and long-time near diffusion are observed, with various time dependences indicated via dashed lines. (b) Corresponding self-intermediate scattering function, $F_s(q,t,t_w)$, measured for $q = 1$. The dashed lines correspond to fits with compressed exponentials and the corresponding β values are indicated.

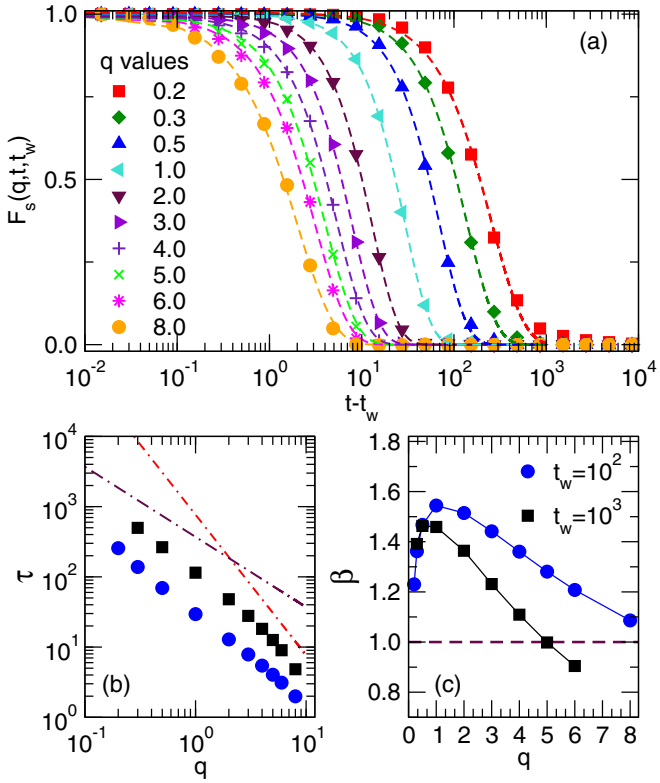

FIG. 3. (a) $F_s(q,t,t_w)$, for different wave vectors q, for $t_w = 10^2$, $T = 0.15$, and $\rho = 0.5$. The dashed lines correspond to compressed exponential fits with fitting parameters reported in (b) and (c) for both $t_w = 10^2$ (circles) and 10^3 (squares).

particle motion depends on t_w, the dynamics being slower for "older" systems, a feature commonly observed in glassy materials. The details of the particle dynamics are, however, intriguing. Except for the very short waiting times where the gel structure is barely formed, four regimes are observed. For $t_w = 10^2$ and 10^3, for instance, the initial ballistic regime is followed by subdiffusive motion, corresponding to particle caging inside the dense glassy domains. Whereas the cage escape is strongly subdiffusive in aging glasses, here we observe instead a remarkable *superdiffusive* particle motion, with $\Delta^2(t,t_w) \approx (t - t_w)^{1.6}$, eventually crossing over to a diffusive regime at very large times (this diffusive regime becomes more evident in larger systems). A superdiffusive regime emerging at large enough time and length scales is observed independent of the choice of damping in the DPD thermostat, demonstrating that it is unrelated to the specific choice of microscopic dynamics, unlike in Refs. [32,33].

We spectrally resolve the dynamics and consider the self-part of the intermediate scattering function $F_s(q,t,t_w) = \frac{1}{N_A}\sum \langle \exp\{i\mathbf{q}\cdot[\mathbf{r}_i(t) - \mathbf{r}_i(t_w)]\}\rangle$ for a given scattering vector $\mathbf{q}$, and for A particles. The data in Fig. 2(b) are for $|\mathbf{q}| = 1$, thus probing the dynamics over a "mesoscopic" length scale of about five particle diameters. The data again display a strong dependence on t_w, with the relaxation slowing down with t_w. The time decay of these correlations can be fitted with a *compressed exponential* form $F_s(q,t,t_w) \approx A \exp[-(\frac{t-t_w}{\tau})^{\beta}]$ with fitting parameters (A,β,τ) which depend both on the age t_w and on the wave vector q. Strikingly, the fitted β values in Fig. 2(b) indicate that $\beta > 1$. There is a faster-than-exponential relaxation process emerging at mesoscopic length scales in the gel, corresponding to the superdiffusive regime in Fig. 2(a). We suspect that finite-size effects affect data for the largest t_w shown, presumably explaining the reduced time window for superdiffusive behavior at large t_w, and the slight decrease in β.

We investigate how the relaxation varies across length scales, by studying the variation of $F_s(q,t,t_w)$ with q in Fig. 3(a) for a given age, $t_w = 10^2$. The corresponding values for the relaxation time τ and the exponent β are shown in Figs. 3(b) and 3(c) for two waiting times. In both cases, a complex behavior is observed. At large q, corresponding to in-cage motion, we find a diffusive process $\tau \sim q^{-2}$ accompanied by stretched exponential relaxations, $\beta < 1$. At larger length scales, a crossover to nearly ballistic dynamics $\tau \sim q^{-\alpha}$ (with $\alpha \approx 1.1$–1.4) is accompanied by compressed exponential $\beta > 1$ with a peak value near $\beta \approx 1.5$ as frequently reported in experiments [23,27]. Eventually, diffusive dynamics and

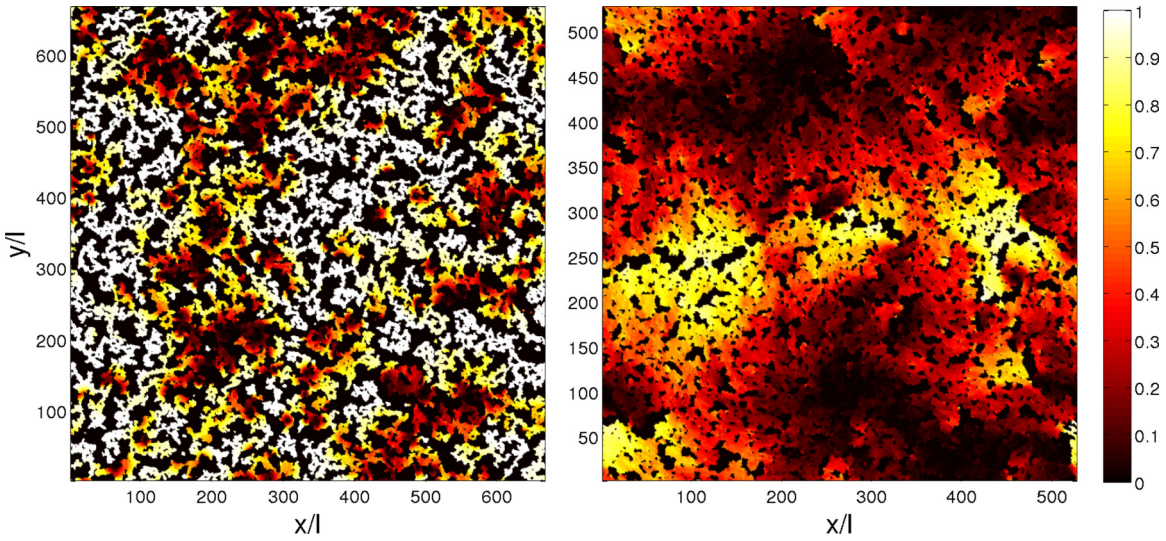

FIG. 4. For $\rho = 0.5$ (left) and 0.8 (right), spatial map of the mobility field, $q(x,y)$, at $t - t_w = 482.74$, for $t_w = 10^2$. Black regions represent empty pores. The typical size of the mobile/immobile domains is much larger than both the particle size and the typical pore size, extending over hundreds of particles, as confirmed in Fig. 5.

exponential relaxation should be recovered at large enough length scales, but these are difficult to access within our numerical simulations.

To visualize the spatiotemporal evolution of the relaxation, we resolve the dynamics for each particle using a mobility function $q_i(t,t_w) = 1 - \exp[-\Delta_i^2(t,t_w)/2a^2]$, such that $q_i(t,t_w) \approx 1$ when the particle's squared displacement $\Delta_i^2(t,t_w) \gg a^2$, and $q_i(t,t_w) \approx 0$ otherwise. We then construct a map of the mobility field $q(\mathbf{r},t,t_w)$ by creating a spatial grid of mesh size 1.5, and averaging q_i over each grid for a given pair (t,t_w). Varying the probe length a allows us to independently consider the various regimes of single-particle dynamics. Our most striking finding is reported in Fig. 4, where we consider the mobility field for $a = 6$ corresponding to the superdiffusive regime and compressed exponential dynamics. These maps reveal that, during the aging process, the local relaxation dynamics is highly heterogeneous and becomes spatially correlated over *ultralong length scales* which are much larger than the typical pore size of the gel.

To quantify the size of these dynamic domains, we measure the spatial correlation function $G_4(r,t,t_w) = \langle \delta q(\mathbf{r}',t,t_w)\delta q(\mathbf{r}+\mathbf{r}',t,t_w)\rangle / \langle \delta q^2(\mathbf{r}',t,t_w)\rangle$, where $\delta q = q - \overline{q}$, with $\overline{\cdots}$ corresponding to a spatial average. Representative data for $G_4(r,t,t_w)$ are shown in Fig. 5. We first show in Figs. 5(a) and 5(b) that the size of correlated domains increases with $t - t_w$ indicating that large-scale correlations develop as the structure reorganizes. In agreement with Fig. 4, the correlations seem longer for larger density. Such large length scales (of more than 100 particle diameters) measured in our simulations are reminiscent of the ultralong correlation lengths measured in experiments using spatially resolved light-scattering techniques [21].

We also observe that the measured correlation lengths, for any $t - t_w$, depend upon the system size. This is seen in Fig. 5(c), where we plot $G_4(r,t,t_w)$ for various system sizes at a given state point. Clearly, the correlation functions decay more slowly for larger systems. If we rescale distances by the linear size of the simulation box, L, there is an approximate collapse of $G_4(r,t,t_w)$ [see Fig. 5(d)]. Such a dependence of the correlations with L suggests that the system size is the only characteristic length scale over which the relaxation is spatially correlated, at least for the system sizes that we can access numerically (our largest L is about 2000 particle diameters). We have employed direct visualization of the gel aging to conclude that these large-scale correlations arise due to the spontaneous elastic recoiling of the network over

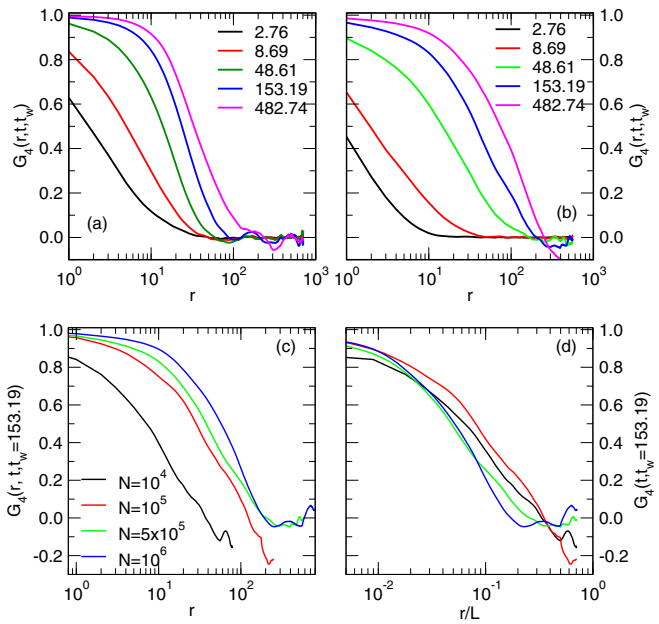

FIG. 5. Spatial correlations of mobility, $G_4(r,t,t_w)$, for different $t - t_w$ (as marked), corresponding to $t_w = 10^2$, at $\rho = 0.5$ (a), 0.8 (b), and (c) for different system sizes (N), as marked, at $\rho = 0.8$, $t_w = 153.19$. (d) Variation of $G_4(r,t,t_w)$ corresponding to (c) with rescaled distances r/L.

large distances after local bonds intermittently break due to thermal activation. These events have been described before [14], but their effect on microscopic dynamics had not been analyzed.

Overall, our large-scale simulations reproduce all anomalous features observed in scattering experiments performed in aging gels, most notably subdiffusive caged dynamics crossing over to superdiffusive, compressed exponential dynamics at large enough length scales characterized by ultra-long-ranged dynamic correlations. In our model, this arises spontaneously because rare localized relaxation events affect the dynamics of the tenuous gel structure over large length scales. Moreover, such aging dynamics is not observed in dense glasses. Although our observations are for a two-dimensional system, the underlying mechanism would also apply for three-dimensional experimental systems, and future numerical work would explore that. Studying the mechanical response of such aging nonequilibrium gels would also be interesting, with a possible interplay of intrinsic and extrinsic time scales. Also, the potential connection to the observation of sudden collapse in many gels after an initial lag time [42] needs exploration. Whether the mechanisms discussed in the context of such low density materials can be extended to understand similar fast relaxations reported for denser aging glasses [43–45] also requires more investigations.

We thank L. Cipelletti and E. Del Gado for useful discussions and the HPC at IMSc for providing the computational facilities. The research leading to these results has received funding from the European Research Council under the European Unions Seventh Framework Programme (FP7/20072013)/ERC Grant Agreement No. 306845. This work was supported by a grant from the Simons Foundation (Grant No. 454933, Ludovic Berthier).

[1] E. Zaccarelli, J. Phys.: Condens. Matter **19**, 323101 (2007).
[2] T. A. Witten, *Structure Fluids* (Oxford University Press, Oxford, 2003).
[3] R. G. Larson, *The Structure and Rheology of Complex Fluids* (Oxford University Press, Oxford, 1999).
[4] E. Del Gado and W. Kob, Phys. Rev. Lett. **98**, 028303 (2007).
[5] P. I. Hurtado, L. Berthier, and W. Kob, Phys. Rev. Lett. **98**, 135503 (2007).
[6] P. Chaudhuri, L. Berthier, P. I. Hurtado, and W. Kob, Phys. Rev. E **81**, 040502(R) (2010).
[7] T. Koyama, T. Araki, and H. Tanaka, Phys. Rev. Lett. **102**, 065701 (2009).
[8] S. Manley, H. M. Wyss, K. Miyazaki, J. C. Conrad, V. Trappe, L. J. Kaufman, D. R. Reichman, and D. A. Weitz, Phys. Rev. Lett. **95**, 238302 (2005).
[9] F. Cardinaux, T. Gibaud, A. Stradner, and P. Schurtenberger, Phys. Rev. Lett. **99**, 118301 (2007).
[10] P. J. Lu, E. Zaccarelli, F. Ciulla, A. B. Schofield, F. Sciortino, and D. A. Weitz, Nature (London) **453**, 499 (2008).
[11] C. P. Royall, S. R. Williams, T. Ohtsuka, and H. Tanaka, Nat. Mater. **7**, 556 (2008).
[12] C. L. Klix, C. P. Royall, and H. Tanaka, Phys. Rev. Lett. **104**, 165702 (2010).
[13] V. Testard, L. Berthier, and W. Kob, Phys. Rev. Lett. **106**, 125702 (2011).
[14] V. Testard, L. Berthier, and W. Kob, J. Chem. Phys. **140**, 164502 (2014).
[15] G. Foffi, C. De Michele, F. Sciortino, and P. Tartaglia, J. Chem. Phys. **122**, 224903 (2005).
[16] G. Foffi, C. De Michele, F. Sciortino, and P. Tartaglia, Phys. Rev. Lett. **94**, 078301 (2005).
[17] L. Cipelletti, L. Ramos, S. Manley, E. Pitard, D. A. Weitz, E. E. Pashkovski, and M. Johansson, Faraday Discuss. **123**, 237 (2003).
[18] L. Cipelletti and L. Ramos, J. Phys.: Condens. Matter **17**, R253 (2005).
[19] J. M. Lynch, G. C. Cianci, and E. R. Weeks, Phys. Rev. E **78**, 031410 (2008).
[20] P. Yunker, Z. Zhang, K. B. Aptowicz, and A. G. Yodh, Phys. Rev. Lett. **103**, 115701 (2009).
[21] A. Duri and L. Cipelletti, Europhys. Lett. **76**, 972 (2006).
[22] L. Cipelletti, S. Manley, R. C. Ball, and D. A. Weitz, Phys. Rev. Lett. **84**, 2275 (2000).
[23] R. Bandyopadhyay, D. Liang, H. Yardimci, D. A. Sessoms, M. A. Borthwick, S. G. J. Mochrie, J. L. Harden, and R. L. Leheny, Phys. Rev. Lett. **93**, 228302 (2004).
[24] H. Guo, S. Ramakrishnan, J. L. Harden, and R. L. Leheny, Phys. Rev. E **81**, 050401 (2010).
[25] D. Orsi, L. Cristofolini, G. Baldi, and A. Madsen, Phys. Rev. Lett. **108**, 105701 (2012).
[26] L. Berthier and G. Biroli, Rev. Mod. Phys. **83**, 587 (2011).
[27] A. Duri, D. A. Sessoms, V. Trappe, and L. Cipelletti, Phys. Rev. Lett. **102**, 085702 (2009).
[28] S. Maccarrone, G. Brambilla, O. Pravaz, A. Duri, M. Ciccotti, J.-M. Fromental, E. Pashkovski, A. Lips, D. A. Sessoms, V. Trappe, and L. Cipelletti, Soft Matter **6**, 5514 (2010).
[29] *Dynamical Heterogeneities in Glasses, Colloids and Granular Materials*, edited by L. Berthier, G. Biroli, J.-P. Bouchaud, L. Cipelletti, and W. van Saarloos (Oxford University Press, Oxford, 2011).
[30] W. Kob and J. L. Barrat, Phys. Rev. Lett. **78**, 4581 (1997).
[31] D. El Masri, L. Berthier, and L. Cipelletti, Phys. Rev. E **82**, 031503 (2010).
[32] S. Saw, N. L. Ellegaard, W. Kob, and S. Sastry, Phys. Rev. Lett. **103**, 248305 (2009).
[33] S. Saw, N. L. Ellegaard, W. Kob, and S. Sastry, J. Chem. Phys. **134**, 164506 (2011).
[34] H. Tanaka and T. Araki, Europhys. Lett. **79**, 58003 (2007).
[35] M. Bouzid, J. Colombo, L. Vieira Barbosa, and E. Del Gado, arXiv:1605.09447.
[36] R. N. Zia, B. J. Landrum, and W. B. Russel, J. Rheol. **58**, 1121 (2014).
[37] J.-P. Bouchaud and E. Pitard, Eur. Phys. J. E **6**, 231 (2001).
[38] E. E. Ferrero, K. Martens, and J.-L. Barrat, Phys. Rev. Lett. **113**, 248301 (2014).
[39] R. Bruning, D. A. St-Onge, S. Patterson, and W. Kob, J. Phys.: Condens. Matter **21**, 035117 (2009).
[40] S. Plimpton, J. Comput. Phys. **117**, 1 (1995).
[41] T. Soddemann, B. Dünweg, and K. Kremer, Phys. Rev. E **68**, 046702 (2003).

[42] P. Bartlett, L. J. Teece, and M. A. Faers, Phys. Rev. E **85**, 021404 (2012).

[43] H. Guo, G. Bourret, M. K. Corbierre, S. Rucareanu, R. B. Lennox, K. Laaziri, L. Piche, M. Sutton, J. L. Harden, and R. L. Leheny, Phys. Rev. Lett. **102**, 075702 (2009).

[44] B. Ruta, Y. Chushkin, G. Monaco, L. Cipelletti, E. Pineda, P. Bruna, V. M. Giordano, and M. Gonzalez-Silveira, Phys. Rev. Lett. **109**, 165701 (2012).

[45] Z. Evenson, B. Ruta, S. Hechler, M. Stolpe, E. Pineda, I. Gallino, and R. Busch, Phys. Rev. Lett. **115**, 175701 (2015).